

Article

Vacuum Brazing of Dissimilar Al 7075 and Al–25 Si Alloy

Dashuang Liu ^{1,2}, Ping Wei ³, Weimin Long ⁴ and Wei Zhou ^{2,*} 

¹ School of Material Science and Engineering, Hefei University of Technology, Hefei 230009, China; dslu@hfut.edu.cn

² School of Mechanical and Aerospace Engineering, Nanyang Technological University, 50 Nanyang Avenue, Singapore 639798, Singapore

³ School of Material Science and Engineering, Jiangsu University of Science and Technology, Zhenjiang 212003, China; semwp@126.com

⁴ Zhengzhou Research Institute of Mechanical Engineering Co., Ltd., Zhengzhou 450001, China; longweimin@camsouth.com.cn

* Correspondence: mwzhou@ntu.edu.sg or wzhou@cantab.net

Abstract: The vacuum brazing of dissimilar Al 7075 and Al–25 Si alloy was investigated. The brazing filler was copper foil with a thickness of 20 µm, and the brazing temperature was 560 °C held for 10 min. The average shear strength of the brazed joint of dissimilar Al 7075 and Al–25 Si alloy was 26.4 MPa. The copper layer was found to be dissolved completely, and the interface of the joint had an irregular shape with a serrated border, indicating a good metallurgical bonding between the two dissimilar alloys. However, factors which might cause deterioration of the shear strength were also observed, including the formation of the intermetallic compounds such as MgZn₂, Cu₂Al and Mg₂Si, the existence of voids and microcracks, the coarsening of grains in Al 7075, and the coarsening of primary Si in Al–25 Si alloy.

Keywords: vacuum brazing; shear strength; Al 7075; Al–25 Si alloy; microstructure



Citation: Liu, D.; Wei, P.; Long, W.; Zhou, W. Vacuum Brazing of Dissimilar Al 7075 and Al–25 Si Alloy. *Metals* **2022**, *12*, 1042. <https://doi.org/10.3390/met12061042>

Academic Editor: Paolo Ferro

Received: 30 April 2022

Accepted: 16 June 2022

Published: 18 June 2022

Publisher's Note: MDPI stays neutral with regard to jurisdictional claims in published maps and institutional affiliations.



Copyright: © 2022 by the authors. Licensee MDPI, Basel, Switzerland. This article is an open access article distributed under the terms and conditions of the Creative Commons Attribution (CC BY) license (<https://creativecommons.org/licenses/by/4.0/>).

1. Introduction

Aluminium alloys are good candidates to replace heavier copper alloys or steels for the purpose of weight reduction in automotive and many other applications [1–3]. Among them, Al 7075 is used in body panels, brake housings, brake pistons, air deflector parts, and seat slides of automobiles because of its high specific strength, low quench sensitivity, wide range of solution heat treatment temperatures and rapid natural aging characteristics [3,4].

SiC ceramic is one of the mainstream human body protection materials. It has the characteristics of low density, high hardness, high bending strength, good bulletproof comprehensive performance, and can maintain the fighter mobility of equipment personnel to a large extent [5]. However, SiC ceramic is brittle and has poor resistance to impact. Joining Al alloy to SiC ceramic would help to overcome this problem. Therefore, the combination of SiC and aluminium alloys, such as Al 7075, has potential engineering applications [5–7].

The challenges in dissimilar alloys welding are the differences of physical and chemical properties between the materials and the formation of intermetallic brittle phases resulting in the degradation of mechanical properties of welds. However, dissimilar materials welding is increasingly demanded from the industry as it can effectively reduce material costs and improve the design [8]. Specifically, the joining between SiC and Al alloys has faced great technical challenges due to the inherent technical difficulty of achieving good bonding between SiC and Al alloys [9]. Yang et al. [10] proposed a new strategy for dissimilar material joining between SiC and Al Alloys by using high-Si Al alloys. Thus, the good connection between high silicon aluminum alloys and 7075 is the key to finally realize the connection between SiC and 7075 aluminum alloys.

It should be noted that more engineering applications require the joining between high silicon aluminum alloys and 7075. The Al-Si alloys are used to fabricate various automobile parts of automobile engine [11] and air conditioning compressors [12], owing to their good thermal conductivity, small coefficient of thermal expansion, light weight, high strength and rigidity [13]. Dissimilar joining between Al-Si and Al 7075 alloys has been required since they are both becoming more common in engineering applications.

The effects of brazing temperature and post weld heat treatment on 7075 alloy brazed joints have been reported [14]. The highest shear strength was 42 MPa when brazed at 600 °C before post weld heat treatment, and then increased obviously when the retrogression temperature was 200 °C. Song et al. [15] investigated contact reactive brazing of Al 7075 alloys using copper layer and the maximum shear strength of 38.7 MPa was obtained when brazing temperature was 600 °C. Copper is chosen as the interlayer to join aluminum alloys because copper and aluminum can have eutectic reaction so as to reduce the brazing temperature and increase the joint strength.

The weldability of an Al 7075 (T6) sheet using the hybrid laser/GMA welding process was examined and the results indicated that a hybrid laser/GMA welding process at the optimized conditions can successfully fusion weld Al 7075 [16]. The Al 7075 alloy has also been welded to join galvanized steel by the cold metal transfer (CMT) welding–brazing process [17], to join titanium alloy (Ti6Al4V) by gas tungsten arc welding (GTAW) [18], and to join a 6061 alloy by friction stir welding (FSW) [19]. Moreover, the interaction behaviors at the interface between a liquid Al–12 Si and solid Ti6Al4V alloy in ultrasonic-assisted brazing in air was investigated [20]. The work by Sekulic et al. [21] has provided empirical evidence needed for an in-depth phenomenological study of dendrite growth phenomena during the brazing of aluminum alloys in the form of composite brazing sheets. The major characteristic of the phenomenon is a sensitivity of the dendrite pattern selection and dendrite population on brazing process parameters, in particular on the temperature during the dwell. The Al–Si alloy has also been welded to join a titanium dissimilar alloy by FSW. In previous research [15], it was reported that the Al 7075 alloy connection was realized by vacuum brazing. The present research work was carried out to study the vacuum brazing of the dissimilar Al 7075 and Al–25Si alloy.

2. Materials and Methods

Table 1 shows the chemical compositions of the two metals to be joined (Al 7075 and Al–25 Si alloy). The hot-rolled Al 7075 and the spray formed Al–25 Si alloy were cut into dimensions of 5 mm × 5 mm × 5 mm and 10 mm × 6 mm × 5 mm, respectively. The specimens were cut from original substrates Al 7075 and Al–25 Si alloy for checking their original microstructures under the optical microscope (OM). The interlayer used was Cu foil of 20 µm in thickness, as shown schematically in Figure 1a. Before brazing, the surfaces of the substrates were polished to eliminate the oxide film. The brazing process was performed using a vacuum aluminum brazing furnace (WZB–10, Zhongshan Kaixuan Vacuum Science & Technology Co., Ltd., Zhongshan, China). The system was capable of maintaining a vacuum of 4.0×10^{-4} Pa at brazing temperature. The heating power was 21 kW and the air cooling pressure was less than 1 bar. At the beginning of the brazing process, the brazing couples were heated to the brazing temperature 560 °C at heating rate of 10 °C/min. Subsequently, the brazing samples were held at 560 °C for 10 min, followed by a furnace cooling.

Table 1. Chemical compositions of the base metals (wt. %).

Alloy	Mg	Zn	Cu	Fe	Si	Mn	Ti	Cr	Al
Al 7075	2.10–2.90	5.10–6.10	1.20–2.00	0.50	0.40	0.30	0.20	0.18–0.28	Bal.
Al–25 Si alloy	1.00	-	4.00	-	25.00	-	-	-	Bal.

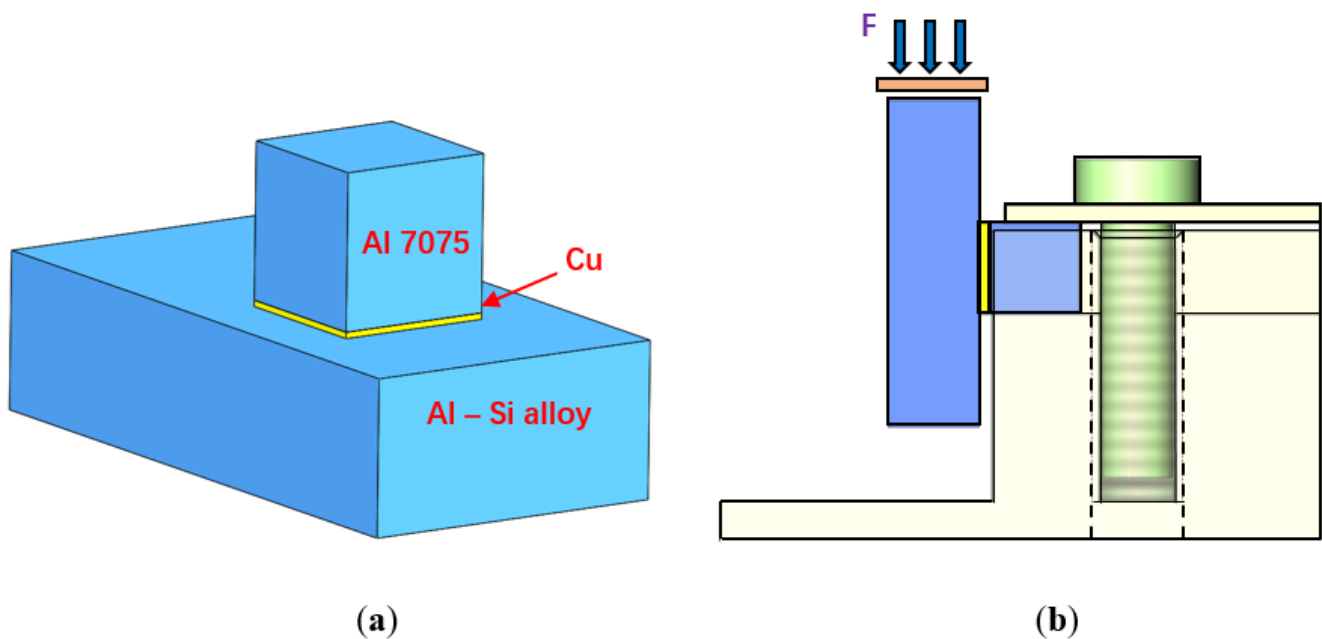


Figure 1. (a) Schematic diagram of assembling brazing parts; (b) Schematic diagram of shear test.

The specimens were cut from the cross section of the brazed joints, polished and etched with the Keller's reagent for 10 s. The microstructure and composition distribution of base metals and brazed joints were characterized by OM, scanning electron microscopy (SEM) and energy dispersive spectrometer (EDS).

The schematic diagram of shear test is shown in Figure 1b. The shear tests were performed at a displacement rate of 0.5 mm/min by a microcomputer controlled electronic universal testing machine (CMT4303, MTS Systems (China) Co., Ltd., Shanghai, China). For each set of experimental data, three specimens were tested to obtain the average shear strength of brazed joints. After shear test, the fracture path and fracture surfaces were characterized under the SEM.

3. Results and Discussion

3.1. Microstructures of Al 7075 and Al-25 Si Alloy before Brazing

Figure 2 shows the microstructures of the Al 7075 and Al-25 Si alloy before (Figure 2a,b) and after (Figure 2c,d) brazing. Figure 3 shows the XRD patterns of the two alloys. The microstructure of Al 7075 consists of Al matrix and $MgZn_2$ precipitates. However, the intensity peak of $MgZn_2$ is small for Al 7075. XRD analysis was also conducted for Al-25 Si alloy and the results indicate the formation of fine Al_2Cu and Mg_2Si precipitates in all the peaks in addition to the existence of Si phase and Al matrix.

Figure 2c,d show the microstructures of the Al 7075 and Al-Si alloy after the brazing process. The sizes of Al grains were found to grow considerably as compared with the original Al 7075 alloy (Figure 2a,b). Moreover, the sizes of primary Si in the Al-25 Si alloy became bigger.

3.2. Microstructures of Brazed Joints of Dissimilar Al 7075 and Al-25 Si Alloy

Figure 4 shows the microstructures of the joint brazed at 560 °C for 10 min. The interface of the joint had an irregular shape with a serrated border, as marked in Figure 4b, which indicates a good metallurgical bonding between the Al 7075 and Al-25 Si alloy. XRD study of the brazed joints shows formation of intermetallic compounds $MgZn_2$, Cu_2Al and Mg_2Si , as shown in Figure 5. While Cu was dissolved in aluminium at the brazing temperature, as the temperature cooled down Al_2Cu was formed, since the solubility of copper in Al was low at room temperature.

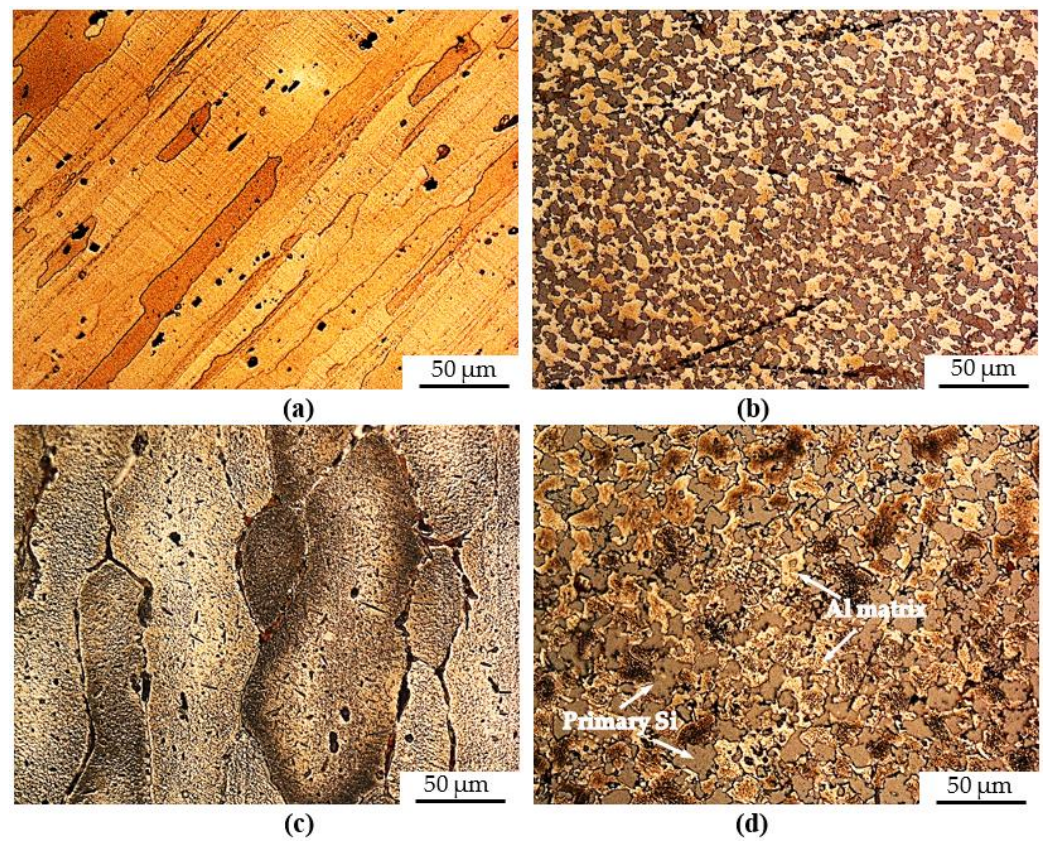
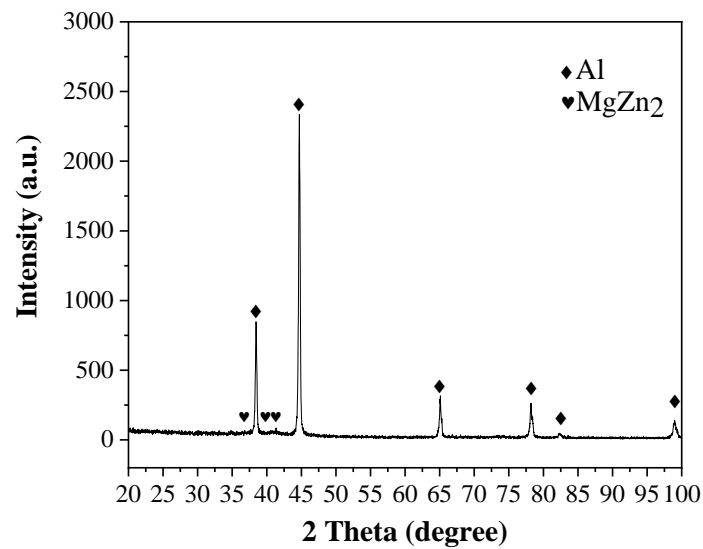
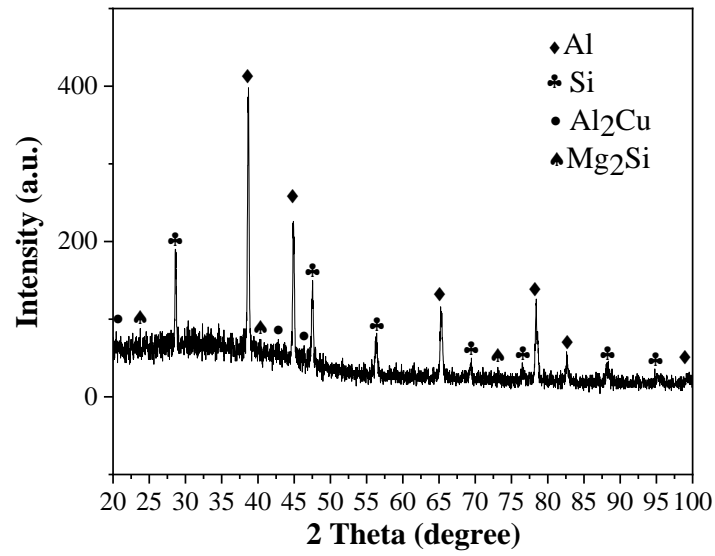


Figure 2. Optical micrographs showing microstructures of Al 7075 and Al-25 Si alloy before and after brazing: (a) Al 7075 before brazing; (b) Al-25 Si alloy before brazing; (c) Al 7075 after brazing; (d) Al-25 Si alloy after brazing.



(a)

Figure 3. Cont.



(b)

Figure 3. The XRD patterns of Al-7075 and Al-Si alloy: (a) Al 7075; (b) Al-25 Si alloy.

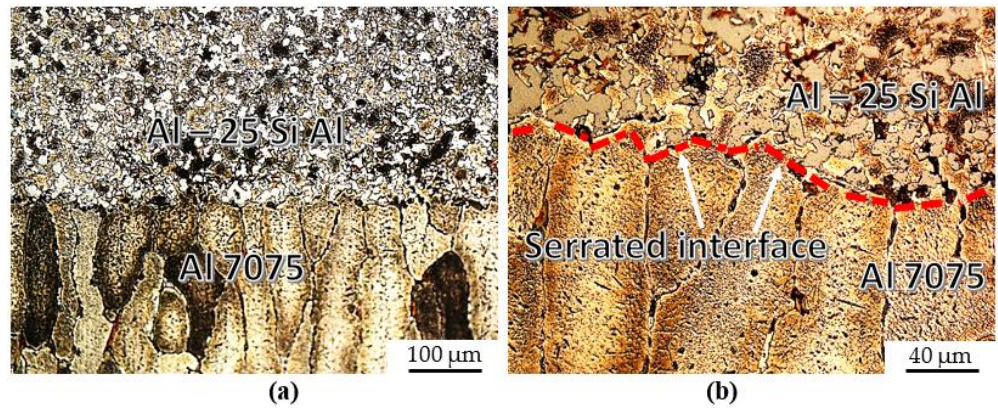


Figure 4. Optical micrographs showing microstructures of the brazed joint at (a) low and (b) higher magnifications.

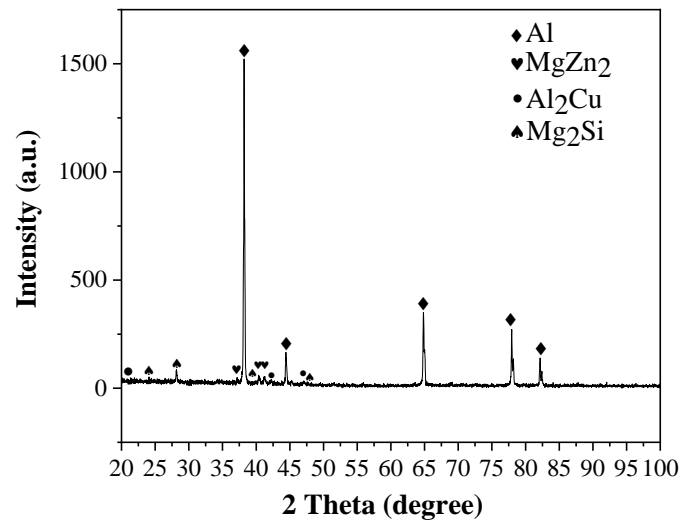


Figure 5. The XRD result of brazed joint of dissimilar Al 7075 and Al-25 Si alloy.

Figure 6 shows the typical distributions of the elements Al, Si, Cu, Zn and Mg in the microstructure. The results show that at the side of the Al 7075 alloy, the microstructure was mainly enriched in Al. In addition, Zn, Cu, and Mg were all detected in the matrix. At the side of the Al-25 Si alloy, the primary precipitates were enriched in Si, and the matrix was enriched in Al. Severe Mg and Cu also existed in the matrix. At the interface between the Al 7075 and Al-25 Si alloy, the Cu foil was not observed. However, there was a very narrow discontinuous region (of about 10–20 μm) where the mapping for Cu was at its most intense. In fact, the presence of Cu extended further. The EDS line-scan analysis, as shown in Figure 7, indicates a similar distribution of elements.

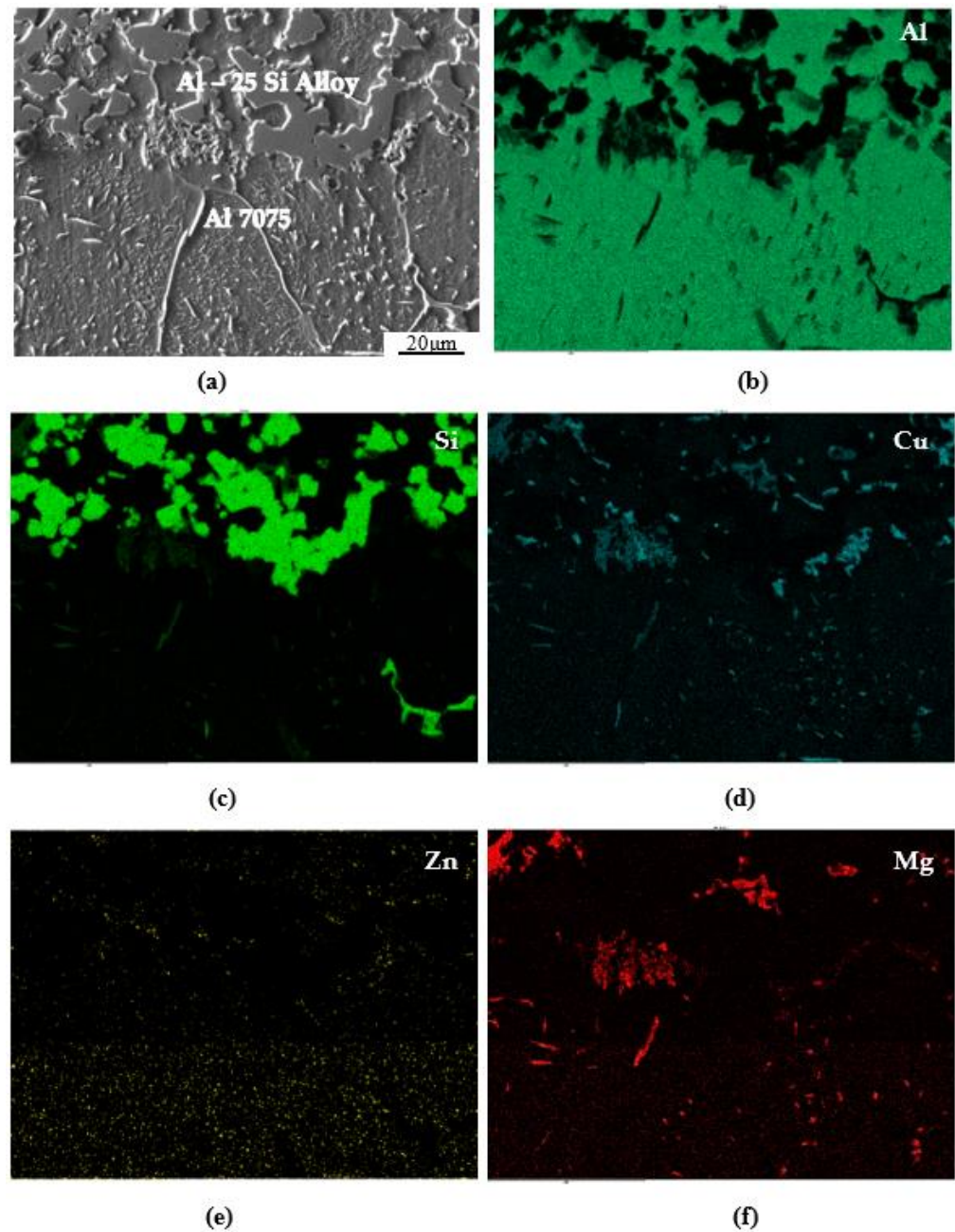
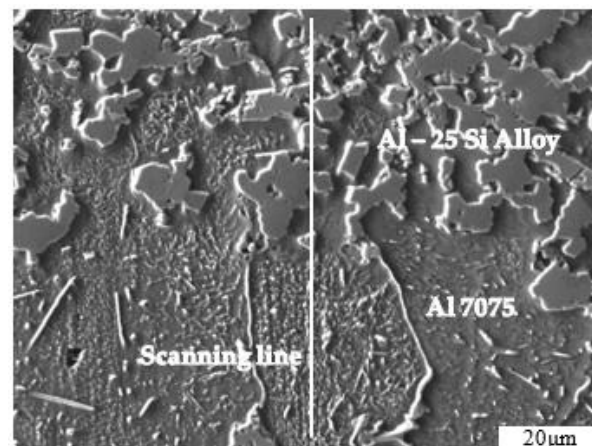
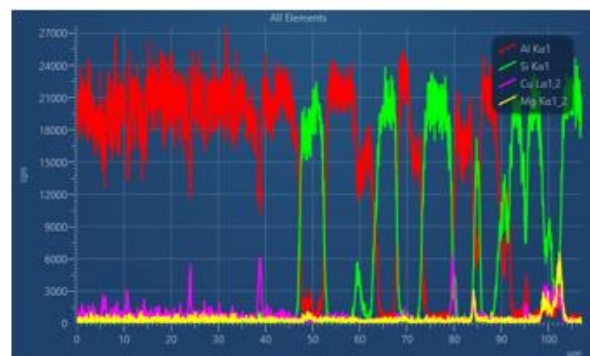


Figure 6. (a) SEM micrograph showing microstructures of the brazed joint. (b–f) EDS mapping of the zone shown in (a) for different alloying elements (Al, Si, Cu, Zn and Mg).



(a)



(b)

Figure 7. (a) SEM micrograph showing microstructures of brazed joint of dissimilar Al 7075 and Al-25 Si alloy; (b) EDS line-scan showing distribution of Cu, Al, Si and Mg across the brazed joint.

Figure 8 shows that there were few cracks and voids in the middle of the brazed joint. Referring to the relevant literature [22], it may be inferred that Al_2O_3 existed in the voids. The oxide film on the surface of the matrix remained in the brazed joint, which led to the generation of void defects. In order to further clarify the element distribution in the void of the brazed joint, EDS map scanning analysis was carried out for a void inside the brazed joint shown in Figure 8c, and distribution of O elements is shown in Figure 8d. The EDS results show that the hole contained O elements, indicating that the oxide film led to the formation of void.

The shear strength of three brazed joints of the dissimilar Al 7075 and Al-25 Si alloy was calculated as the ratio of the maximum shear force to the area of the shear plane and found to be 23.9 MPa, 34.7 MPa, and 20.6 MPa, respectively. Thus, the average shear strength of the brazed joint was 26.4 MPa. All the brazed joints fractured at the joint interface, indicating an adhesive failure mode.

Figure 9 shows the micrographs of fractures at the Al 7075 alloy side of the brazed joints. The fracture analyses for three samples were performed to study the fracture mode of the joint. From Figure 9a, a small number of shallow dimples were observed on the fracture surface. The average dimple depth was approximately 200 μm . The similar results were observed in Figure 9b,c. The micrographs of fracture surfaces of brazed joints (see Figure 9) and the lower hardness values indicated the brittle fracture characteristics and the low toughness of brazing joints of the dissimilar Al 7075 and Al-25 Si alloy.

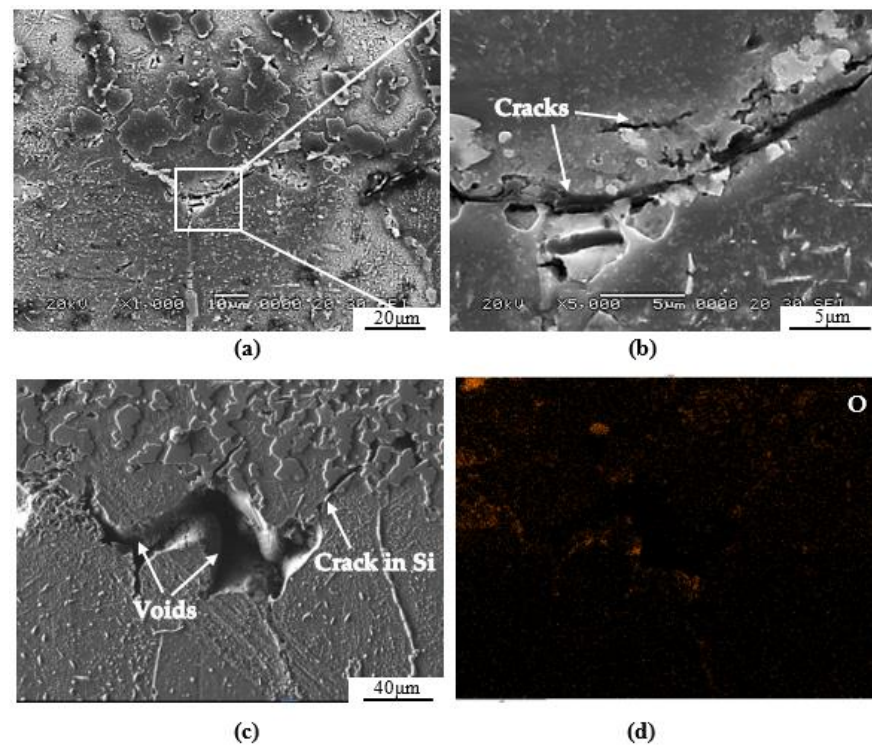


Figure 8. Voids in the middle of the brazed joint: (a) Crack existed in the joint; (b) Magnification of (a); (c) Void existed in the joint; (d) The distribution of O element in void shown in (c).

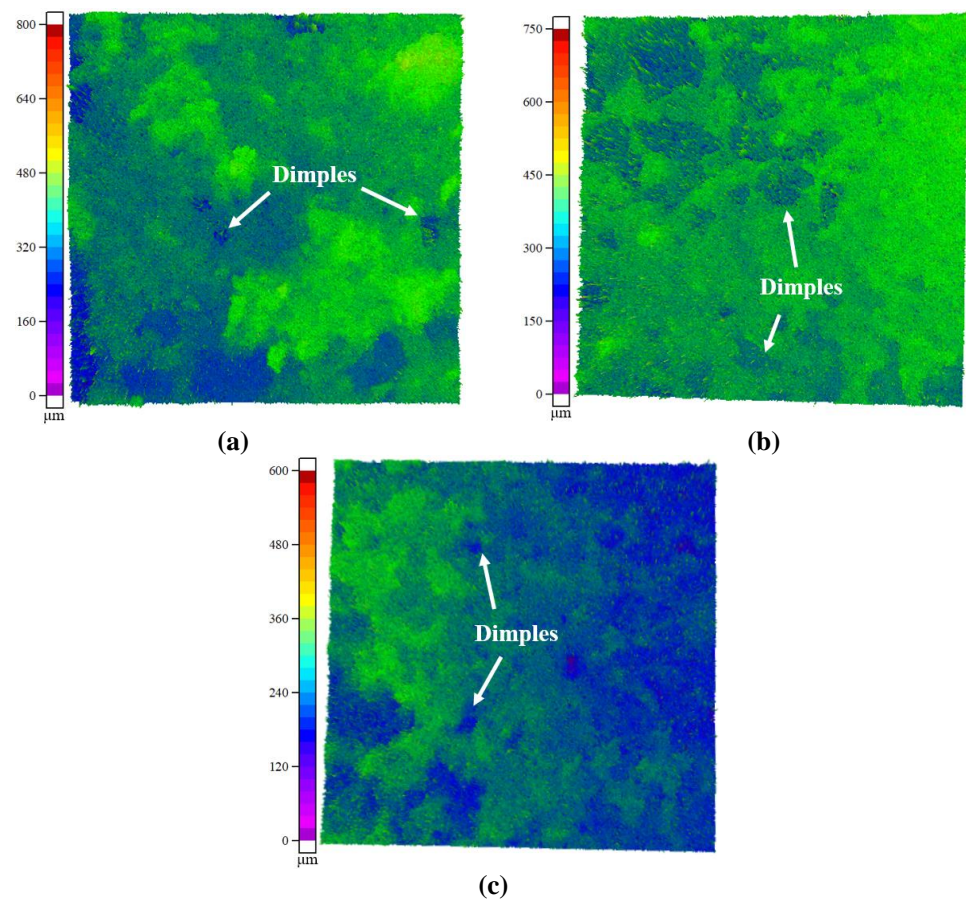


Figure 9. Micrographs of fractures of brazed joints showing a small amount of shallow dimples in three samples in (a–c).

4. Discussion

According to the Al–Cu binary diagram, at a brazing temperature higher than that of Al–Cu eutectic reaction (TE: 548.2 °C), the eutectic liquid phase will be formed by Al–Cu eutectic reaction, to realize the joining of an aluminum alloy. Therefore, the Cu was utilized to react with the alloy constituents to form an interlayer to join the Al 7075 and Al–25 Si alloy and the brazing temperature (TB) was determined as 560 °C.

Figure 10 shows schematically the mechanism of vacuum brazing between the dissimilar Al 7075 and Al–25 Si alloy. When the temperature was less than TE in the heating process, there is only the mutual diffusion between Al and Cu atoms, as shown in Figure 10a. Due to the fact that diffusion rate of a Cu atom in Al is higher than that of an Al atom in Cu, a large number of Cu atoms preferentially diffused to the aluminum alloy matrix and produced diffusion gradient, leading to the formation of different diffusion transition layers.

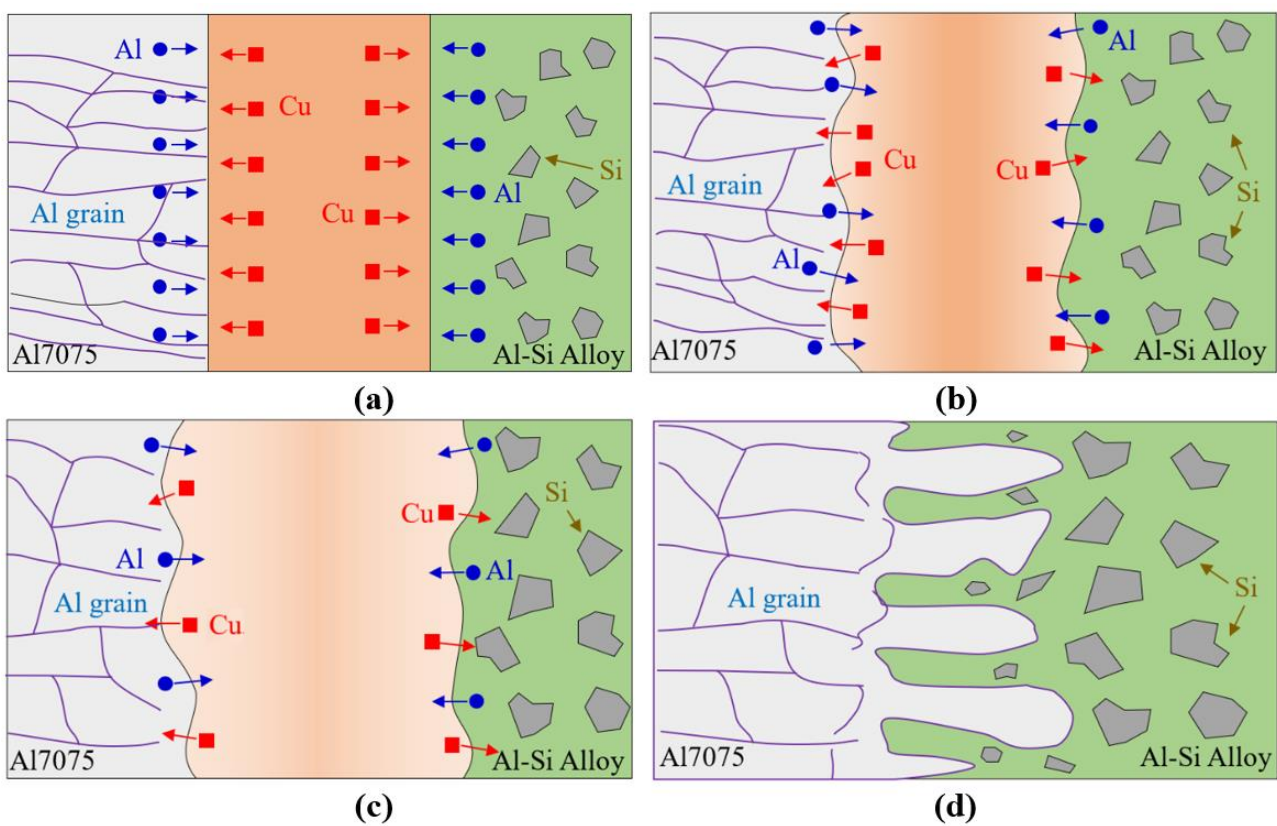


Figure 10. Schematic diagram showing formation mechanism of vacuum brazing joint between the dissimilar Al 7075 and Al–25 Si alloy: (a) Solid—phase atomic diffusion reaction stage; (b) Liquid phase generation and expansion stages; (c) Liquid phase homogenization stage; (d) Cooling stage.

When the temperature \geq TE (548.2 °C), Cu diffused into the aluminum alloy matrix to form a solid solution, leading to the gradual decrease of α -Al melting point. Thus, the eutectic liquid phase was formed at the interface of the aluminum alloy matrix with the increasing of temperature. The dissolution of Al and Cu was accelerated to the liquid phase, and then the width of eutectic liquid phase increased gradually until the intermediate Cu middle layer completely reacted and dissolved (Figure 10b).

When the temperature was increased up to TB (560 °C) and then held for 10 min at TB temperature, the Cu atoms in the liquid phase continued to diffuse to both sides of matrix, and the Al continued to be dissolved to the liquid phase, resulting in the continuous increase of the liquid phase width. At the same time, the composition of the liquid phase was homogenized by atomic diffusion to reduce the inhomogeneous composition and concentration gradient of the eutectic liquid phase (Figure 10c).

In the subsequent slow cooling process, the composition of Cu in the liquid phase side of the interface gradually decreased because of the diffusion of Cu atoms into the matrix, resulting in the increase of the melting point of the liquid phase and the isothermal solidification of the liquid phase at the interface and the formation of α -Al solid solution. At this stage, the width of the liquid phase gradually decreased until the complete isothermal solidification of the liquid phase.

However, the holding time used in this paper was not enough to complete the isothermal solidification process of the liquid phase. Thus, it had entered the cooling stage before the isothermal solidification of the eutectic liquid phase was completed. The residual liquid phase undergoes cooling solidification and reacts to form intermetallic compounds Al_2Cu (Figure 10d). In the whole brazing process, both Al grains in Al 7075 and primary Si in Al-25 Si alloy grew drastically in size owing to the cumulative heating effects, as shown in Figure 2.

Figure 10 shows schematically a broad picture of the brazing process with the major features only and there is room for further improvement when better understanding is obtained through further research in the future.

From the microstructural investigation, there was a good bonding between the Al 7075 and Al-25 Si alloy (Figures 4, 6 and 7). However, the shear strength was about 26.4 MPa, which was less than that of the base metal Al 7075 or Al-25 Si alloy. Several reasons for the degradation of the shear strength could be listed. First, the precipitation of the intermetallic compound such as MgZn_2 , Cu_2Al and Mg_2Si , contributed to the brittleness of brazing joints of the dissimilar Al 7075 and Al-25 Si alloy. Secondly, the existence of voids and cracks reduced the shear strength. Thirdly, the coarsening of the size of an Al grain of Al 7075 and the size of the primary Si of Al-25 Si alloy led to the reduction of the mechanical properties of the joints.

5. Conclusions

- (1) The vacuum brazing of the dissimilar Al 7075 and Al-25 Si alloy was performed for the first time. The brazing filler was copper foil with a thickness of 20 μm , and the brazing temperature was 560 $^\circ\text{C}$ held for 10 min. The average shear strength of the brazed joint of the dissimilar Al 7075 and Al-25 Si alloy was 26.4 MPa.
- (2) The copper layer was dissolved completely, and the interface of the joint had an irregular shape with a serrated border, indicating a good metallurgical bonding between the Al 7075 and Al-25 Si alloy.
- (3) The precipitation of the intermetallic compounds such as MgZn_2 , Cu_2Al and Mg_2Si , the existence of voids and cracks, and the coarsening of the sizes of Al grains in Al 7075 and the sizes of primary Si in Al-25 Si alloy, contributed to a deteriorated shear strength of the brazed joint of dissimilar Al 7075 and Al-25 Si alloy.

Author Contributions: Conceptualization, D.L. and W.Z.; methodology, D.L., W.L. and W.Z.; validation, P.W.; formal analysis, D.L., P.W. and W.Z.; investigation, D.L., P.W. and W.L.; data curation, D.L. and P.W.; writing—original draft preparation, D.L., P.W. and W.L.; writing—review and editing, D.L. and W.Z.; visualization, D.L. and P.W.; supervision, W.L. and W.Z.; project administration, W.L. and W.Z.; funding acquisition, D.L. and W.Z. All authors have read and agreed to the published version of the manuscript.

Funding: This research was funded by Ministry of Defence (MINDEF), Singapore through grant #001498-00008. This work was also supported by China Postdoctoral Science Foundation Funded Project (Grant No. 2016M601753), Funding of National Natural Science Foundation of China (Grant No. 51405208), Machinery Science Research Institute Group Co., Ltd. Technology Development Fund Project (Grant No. AZXJJ2031903), Major Projects of Natural Science Research in Colleges and Universities in Jiangsu (Grant No. 19KJA460009) and Postdoctoral International Exchange Program (Dispatch Project).

Institutional Review Board Statement: Not applicable.

Informed Consent Statement: Not applicable.

Data Availability Statement: Not applicable.

Conflicts of Interest: The authors declare no conflict of interest.

References

1. Miller, W.S.; Zhuang, L.; Bottema, J.; Wittebrood, A.J.; Smet, P.D.; Haszler, A.; Vieregge, A. Recent development in aluminium alloys for the automotive industry. *Mater. Sci. Eng. A* **2020**, *280*, 37–49. [[CrossRef](#)]
2. Liu, D.S.; Wei, P.; Long, W.M.; Zhou, W.; Zhou, W.; Wang, J.Y. Effect of welding wires on fatigue property of 7n01-T4 aluminium alloy joints. *Sci. Technol. Weld. Join.* **2020**, *1*, 1–10. [[CrossRef](#)]
3. Langebeck, A.; Bohlen, A.; Freisse, H.; Vollertsen, F. Additive manufacturing with the lightweight material aluminium alloy EN AW-7075. *Weld. World* **2019**, *64*, 429–436. [[CrossRef](#)]
4. Rafi, H.K.; Ram, G.D.J.; Phanikumar, G.; Rao, K.P. Microstructure and tensile properties of friction welded aluminum alloy AA7075-T6. *Mater. Des.* **2010**, *31*, 2375–2380. [[CrossRef](#)]
5. He, R.; Zhou, N.; Zhang, K.; Zhang, X.; Fang, D. Progress and challenges towards additive manufacturing of SiC ceramic. *J. Adv. Ceram.* **2021**, *10*, 637–674. [[CrossRef](#)]
6. Sozhamannan, G.G.; Prabu, S.B. Influence of interface compounds on interface bonding characteristics of aluminium and silicon carbide. *Mater. Charact.* **2009**, *60*, 986–990. [[CrossRef](#)]
7. Lin, Y.C.; McGinn, P.J.; Mukasyan, A.S. High temperature rapid reactive joining of dissimilar materials: Silicon carbide to an aluminum alloy. *J. Eur. Ceram. Soc.* **2012**, *32*, 3809–3818. [[CrossRef](#)]
8. Chen, H.C.; Pinkerton, A.J.; Lin, L. Fibre laser welding of dissimilar alloys of Ti-6Al-4V and Inconel 718 for aerospace applications. *Int. J. Adv. Manuf. Technol.* **2011**, *52*, 977–987. [[CrossRef](#)]
9. Teng, P.; Li, X.; Hua, P.; Liu, H.; Wang, G. Effect of metallization temperature on brazing joints of SiC ceramics and 2219 aluminum alloy. *Int. J. Appl. Ceram. Technol.* **2022**, *19*, 498–507. [[CrossRef](#)]
10. Yang, Y.; Bhowmik, A.; Tan, J.L.; Du, Z.; Zhou, W. A new strategy for dissimilar material joining between SiC and Al alloys through use of high-Si Al alloys. *Metals* **2022**, *12*, 887. [[CrossRef](#)]
11. Hayashi, T.; Takada, Y. Spray formed aluminum alloy finds engine role. *Met. Powder Rep.* **1991**, *46*, 23. [[CrossRef](#)]
12. Hayashi, T.; Takeda, Y.; Akechi, K.; Fujiwara, T. Rotary car air conditioner made with PM Al-Si wrought alloys. *Met. Powder Rep.* **1991**, *46*, 23–29. [[CrossRef](#)]
13. Zou, Q.; Han, N.; Zhang, Z.; Jie, J.; An, X. Enhancing segregation behavior of impurity by electromagnetic stirring in the solidification process of Al-30Si Alloy. *Metals* **2020**, *10*, 155. [[CrossRef](#)]
14. Niu, C.N.; Song, X.G.; Hu, S.P.; Lu, G.Z.; Chen, Z.B.; Wang, G.D. Effects of brazing temperature and post weld heat treatment on 7075 alloy brazed joints. *J. Mater. Process. Tech.* **2019**, *266*, 363–372. [[CrossRef](#)]
15. Song, X.G.; Niu, C.N.; Hu, S.P.; Liu, D.; Cao, J.; Feng, J.C. Contact reactive brazing of Al7075 alloy using Cu layer deposited by magnetron sputtering. *J. Mater. Process. Tech.* **2018**, *252*, 469–476. [[CrossRef](#)]
16. Hu, B.; Richardson, I.M. Hybrid laser/GMA welding aluminium alloy 7075. *Weld. World* **2006**, *50*, 51–57. [[CrossRef](#)]
17. Qin, Y.; He, X.; Jiang, W. Influence of preheating temperature on cold metal transfer (CMT) welding—brazing of aluminium alloy / galvanized steel. *App. Sci.* **2018**, *8*, 1659. [[CrossRef](#)]
18. Nandagopal, K.; Kailasanathan, C. Analysis of mechanical properties and optimization of gas tungsten arc welding (GTAW) parameters on dissimilar metal titanium (6Al4V) and aluminium 7075 by Taguchi and ANOVA techniques. *J. Alloys Compd.* **2016**, *682*, 503–516. [[CrossRef](#)]
19. Ravikumar, S.; Rao, V.S.; Pranesh, R.V. Effect of process parameters on mechanical properties of friction stir welded dissimilar materials between AA6061-T651 and AA7075-T651 alloys. *Int. J. Adv. Mech. Eng.* **2014**, *4*, 101–114.
20. Chen, X.; Yan, J.; Gao, F.; Wei, J.; Xu, Z.; Fan, G. Interaction behaviors at the interface between liquid Al-Si and solid Ti-6Al-4V in ultrasonic-assisted brazing in air. *Ultrason. Sonochem.* **2013**, *20*, 144–154. [[CrossRef](#)]
21. Sekulic, D.P.; Galenko, P.K.; Krivilyov, M.D.; Krivilyov, C.; Walker, L.; Gao, F. Dendritic growth in Al-Si alloys during brazing. Part 1: Experimental evidence and kinetics. *Int. J. Heat Mass Trans.* **2005**, *48*, 2372–2384. [[CrossRef](#)]
22. Yousefi Mehr, V.; Toroghinejad, M.R.; Rezaeian, A. The effects of oxide film and annealing treatment on the bond strength of Al-Cu strips in cold roll bonding process. *Mater. Des.* **2014**, *53*, 174–181. [[CrossRef](#)]